The Process of Tholin Formation in Titan's Upper Atmosphere

J. H. Waite, Jr., *et al.*

Science **316**, 870 (2007);
DOI: 10.1126/science.1139727

Science (print ISSN 0036-8075; online ISSN 1095-9203) is published weekly, except the last week in December, by the American Association for the Advancement of Science, 1200 New York Avenue NW, Washington, DC 20005.

momentum. Furthermore, a sudden onset of interactions would likely affect the density distribution of the minority atoms. However, the minority clouds observed in expansion are well fit by a single Thomas-Fermi profile (*25*).

The BEC-side picture of a mixture of single atoms and molecules seems to extend into the resonance region, in the sense that fermion pairs form high above the superfluid transition temperature and possibly coexist locally with unpaired atoms. However, the fermion pairs on resonance behave differently from "real" molecules: Their binding energy increases with lower temperature and higher atomic density. Most important, fermion pairs above the CC limit do not condense at low temperature as bosonic molecules would do at any imbalance. Although some extensions of BCS mean-field theories to the imbalanced case do not predict pairing at imbalances δ above the CC limit (*26*), a survival of Cooper pairs "far from the transition region" has been predicted (*27*) for a superconducting system that is driven into the normal, paramagnetic phase by Zeeman splitting.

The observed spectral gaps appear to be insensitive to the density of the minority atoms (Fig. 4, A to C). At very high imbalances, one should indeed approach the limit of one minority atom immersed in a fully polarized Fermi sea. In (*24*, *28*, *29*) the ground-state energy for this scenario has been calculated to be about $-0.6E_F$, for example, by using a modified Cooper-pair wave function ansatz (*28*). These calculations do not provide an excitation spectrum and do not distinguish between pairing (correlation) energies and mean-field (Hartree) terms. Therefore, the theoretical result cannot be directly compared to our spectroscopic measurement of $h\Delta\nu = -0.38E_F$ at $T/T_F = 0.08$.

Whether superfluidity can occur for large imbalances and low atom numbers in highly elongated geometries remains a subject of debate (*30*). In light of our findings, it may be important to clearly distinguish between the effects of pairing and of superfluidity. It has also been suggested that the presence of an atomic peak next to the pairing peak in the minority cloud at zero temperature and high imbalance could provide evidence for exotic forms of superfluidity, such as the Fulde-Ferrel-Larkin-Ovchinnikov state (*31*). However, for the parameters studied here, the atomic peak is seen to disappear as the temperature is reduced (Figs. 2 and 4A).

Working with imbalanced Fermi gases, we were able to study and characterize pairing in a situation where no superfluidity occurs even at zero temperature. The spectral gap $\Delta\nu$ appears to be only weakly dependent on the imbalance. This finding suggests that near unitarity, certain pairing correlations in the superfluid state are similar to those in a dilute cloud of minority atoms immersed into the Fermi sea of the majority. Moreover, it implies that the energetics that drive the normal-to-superfluid phase transition involve more than the observed pairing energy. Further studies of the strongly correlated normal state might yield new insights into the microscopic physics of the superfluid state.

References and Notes

1. P. A. Lee, N. Nagaosa, X.-G. Wen, *Rev. Mod. Phys.* **78**, 17 (2006).
2. M. W. Zwierlein, J. R. Abo-Shaeer, A. Schirotzek, C. H. Schunck, W. Ketterle, *Nature* **435**, 1047 (2005).
3. N. Trivedi, M. Randeria, *Phys. Rev. Lett.* **75**, 312 (1995).
4. A. Perali, P. Pieri, G. C. Strinati, C. Castellani, *Phys. Rev. B* **66**, 024510 (2002).
5. Q. Chen, J. Stajic, S. Tan, K. Levin, *Phys. Rep.* **412**, 1 (2005).
6. C. Chin *et al.*, *Science* **305**, 1128 (2004); published online 22 July 2004 (10.1126/science.1100818).
7. J. Kinnunen, M. Rodríguez, P. Törmä, *Science* **305**, 1131 (2004); published online 22 July 2004 (10.1126/science.1100782).
8. B. S. Chandrasekhar, *Appl. Phys. Lett.* **1**, 7 (1962).
9. A. M. Clogston, *Phys. Rev. Lett.* **9**, 266 (1962).
10. K. Capelle, *Phys. Rev. B* **65**, 100515 (2002).
11. M. Maśka, *Phys. Rev. B* **66**, 054533 (2002).
12. K. Kumagai *et al.*, *Phys. Rev. Lett.* **97**, 227002 (2006).
13. M. W. Zwierlein, A. Schirotzek, C. H. Schunck, W. Ketterle, *Science* **311**, 492 (2006); published online 21 December 2005 (10.1126/science.1122318).
14. C. A. Regal, M. Greiner, D. S. Jin, *Phys. Rev. Lett.* **92**, 040403 (2004).
15. M. W. Zwierlein *et al.*, *Phys. Rev. Lett.* **92**, 120403 (2004).
16. Z. Hadzibabic *et al.*, *Phys. Rev. Lett.* **91**, 160401 (2003).
17. Y. Shin, M. W. Zwierlein, C. H. Schunck, A. Schirotzek, W. Ketterle, *Phys. Rev. Lett.* **97**, 030401 (2006).
18. S. Gupta *et al.*, *Science* **300**, 1723 (2003); published online 8 May 2003 (10.1126/science.1085335).
19. See supporting material on *Science* Online.
20. J. Kinnunen, M. Rodríguez, P. Törmä, *Phys. Rev. Lett.* **92**, 230403 (2004).
21. Y. Ohashi, A. Griffin, *Phys. Rev. A* **72**, 063606 (2005).
22. Y. He, Q. Chen, K. Levin, *Phys. Rev. A* **72**, 011602 (2005).
23. Z. Yu, G. Baym, *Phys. Rev. A* **73**, 063601 (2006).
24. C. Lobo, A. Recati, S. Giorgini, S. Stringari, *Phys. Rev. Lett.* **97**, 200403 (2006).
25. M. W. Zwierlein, C. H. Schunck, A. Schirotzek, W. Ketterle, *Nature* **442**, 54 (2006).
26. C. Chien, Q. Chen, Y. He, K. Levin, *Phys. Rev. Lett.* **98**, 110404 (2007).
27. I. L. Aleiner, B. L. Altshuler, *Phys. Rev. Lett.* **79**, 4242 (1997).
28. F. Chevy, *Phys. Rev. A* **74**, 063628 (2006).
29. A. Bulgac, M. M. Forbes, *Phys. Rev. A* **75**, 031605(R) (2007).
30. G. B. Partridge *et al.*, *Phys. Rev. Lett.* **97**, 190407 (2006).
31. J. Kinnunen, L. M. Jensen, P. Törmä, *Phys. Rev. Lett.* **96**, 110403 (2006).

32. We thank W. Zwerger, P. Lee, K. Levin, and Q. Chen for stimulating discussions and D. Miller for critical reading of the manuscript. Supported by NSF and the Office of Naval Research.

Supporting Online Material

www.sciencemag.org/cgi/content/full/316/5826/867/DC1
Materials and Methods
Figs. S1 to S3
References

2 February 2007; accepted 29 March 2007
10.1126/science.1140749

The Process of Tholin Formation in Titan's Upper Atmosphere

J. H. Waite Jr.,[1]* D. T. Young,[1] T. E. Cravens,[2] A. J. Coates,[3] F. J. Crary,[1] B. Magee,[1]* J. Westlake[4]

Titan's lower atmosphere has long been known to harbor organic aerosols (tholins) presumed to have been formed from simple molecules, such as methane and nitrogen (CH_4 and N_2). Up to now, it has been assumed that tholins were formed at altitudes of several hundred kilometers by processes as yet unobserved. Using measurements from a combination of mass/charge and energy/charge spectrometers on the Cassini spacecraft, we have obtained evidence for tholin formation at high altitudes (~1000 kilometers) in Titan's atmosphere. The observed chemical mix strongly implies a series of chemical reactions and physical processes that lead from simple molecules (CH_4 and N_2) to larger, more complex molecules (80 to 350 daltons) to negatively charged massive molecules (~8000 daltons), which we identify as tholins. That the process involves massive negatively charged molecules and aerosols is completely unexpected.

Methane and nitrogen in Titan's atmosphere are supplied with free energy from solar ultraviolet (UV) radiation and energetic particles in Saturn's magnetosphere. These circumstances make Titan, a prolific source of complex organic compounds, unparalleled in the solar system. Hydrocarbon chemistry is further enhanced by the escape of hydrogen from the exosphere, which accelerates the conversion of methane to unsaturated hydrocarbon-nitrile species by circumventing the buildup of molecular hydrogen, thus promoting unsaturated hydrocarbon formation (*1*, *2*). Sagan and Khare (*3*) have suggested that the penultimate result of the formation of these large compounds is the generation of hydrocarbon-nitrile aerosols (tholins) thought to populate haze layers in Titan's stratosphere (*4*, *5*). Similar organic chemistry occurs during soot formation in Earth's troposphere (*6*–*8*) and may have taken place in the

[1]Space Science and Engineering Division, Southwest Research Institute (SWRI), 6220 Culebra Road, San Antonio, TX 78238, USA. [2]Department of Physics and Astronomy, University of Kansas, Lawrence, KS 66045, USA. [3]Department of Space and Climate Physics, Mullard Space Science Laboratory, University College London, Holmbury St. Mary, Dorking RH5 6NT, UK. [4]Department of Physics and Astronomy, University of Texas, San Antonio, TX 78249, USA.

*To whom correspondence should be addressed. E-mail: hwaite@swri.edu (J.H.W.); bmagee@swri.edu (B.M.)

Table 1. INMS observed neutral mole fractions at closest approach. Mole fractions are found from inbound observations within 15 km of closest approach to maximize signal and reduce contamination. Uncertainties are shown in parentheses. H_2 values for all flybys [4.05×10^{-3} (3.00×10^{-5})] have been adopted from analysis of the first Cassini encounter with Titan (TA). Temperature values are obtained from the scale height of N_2 measured within 100 km of closest approach. SZA, solar zenith angle.

	T16	T17	T18	T19	T20	T21	T23
Total density (cm^{-3})	1.78×10^{10} (5.33×10^{6})	5.39×10^{9} (3.04×10^{6})	1.06×10^{10} (4.18×10^{6})	7.10×10^{9} (3.45×10^{6})	3.28×10^{9} (3.33×10^{6})	7.23×10^{9} (3.46×10^{6})	7.66×10^{9} (3.49×10^{6})
N_2	0.975 (3.52×10^{-4})	0.965 (9.64×10^{-3})	0.971 (4.56×10^{-4})	0.968 (5.47×10^{-4})	0.968 (1.13×10^{-3})	0.971 (5.37×10^{-4})	0.975 (5.36×10^{-4})
CH_4	0.0127 (3.18×10^{-5})	0.0241 (7.69×10^{-5})	0.0155 (4.59×10^{-5})	0.0213 (6.46×10^{-5})	0.0193 (1.27×10^{-4})	0.0184 (5.89×10^{-5})	0.0137 (5.03×10^{-5})
C_2H_2	2.05×10^{-4} (3.07×10^{-6})	2.60×10^{-4} (6.04×10^{-6})	2.52×10^{-4} (4.43×10^{-6})	2.03×10^{-4} (4.77×10^{-6})	2.51×10^{-4} (1.10×10^{-5})	2.04×10^{-4} (4.69×10^{-6})	2.24×10^{-4} (4.89×10^{-6})
C_2H_4	6.80×10^{-4} (6.02×10^{-6})	1.01×10^{-3} (1.28×10^{-5})	7.15×10^{-4} (8.04×10^{-6})	9.93×10^{-4} (1.14×10^{-5})	7.69×10^{-4} (2.06×10^{-5})	7.33×10^{-4} (9.58×10^{-6})	8.31×10^{-4} (1.02×10^{-5})
C_2H_6	1.66×10^{-5} (8.52×10^{-7})	1.06×10^{-5} (1.19×10^{-6})	2.04×10^{-5} (1.23×10^{-6})	9.68×10^{-6} (1.02×10^{-6})	1.26×10^{-5} (2.39×10^{-6})	8.74×10^{-6} (9.47×10^{-7})	1.17×10^{-5} (1.09×10^{-6})
C_3H_4	1.21×10^{-5} (6.81×10^{-7})	9.61×10^{-6} (1.06×10^{-6})	1.09×10^{-5} (8.39×10^{-7})	1.08×10^{-5} (1.01×10^{-6})	7.23×10^{-6} (1.69×10^{-6})	7.26×10^{-6} (8.06×10^{-7})	1.21×10^{-5} (1.04×10^{-6})
C_4H_2	4.58×10^{-6} (3.97×10^{-7})	3.95×10^{-6} (6.44×10^{-7})	5.05×10^{-6} (5.43×10^{-7})	5.81×10^{-6} (6.99×10^{-7})	3.96×10^{-6} (1.19×10^{-6})	2.33×10^{-6} (4.34×10^{-7})	5.86×10^{-6} (6.85×10^{-7})
C_2N_2	3.51×10^{-6} (5.43×10^{-7})	4.53×10^{-6} (1.08×10^{-6})	3.30×10^{-6} (6.86×10^{-7})	5.81×10^{-6} (1.09×10^{-6})	4.16×10^{-6} (1.91×10^{-6})	2.43×10^{-6} (6.92×10^{-7})	5.16×10^{-6} (1.01×10^{-6})
C_6H_6	4.39×10^{-6} (3.21×10^{-7})	1.35×10^{-6} (3.11×10^{-7})	3.30×10^{-6} (3.62×10^{-7})	2.42×10^{-6} (3.72×10^{-7})	1.55×10^{-6} (6.14×10^{-7})	1.07×10^{-6} (2.42×10^{-7})	5.07×10^{-6} (5.25×10^{-7})
C_3H_6	4.00×10^{-6} (4.29×10^{-7})	1.83×10^{-6} (5.07×10^{-7})	2.72×10^{-6} (4.61×10^{-7})	2.03×10^{-6} (4.78×10^{-7})	1.55×10^{-6} (8.61×10^{-7})	1.75×10^{-6} (4.53×10^{-7})	3.02×10^{-6} (5.69×10^{-7})
Altitude (km)	950	1000	960	980	1030	1000	1000
Latitude	85°	23°	71°	61°	7.5°	44°	31°
SZA	105°	45°	90°	81°	25°	124°	53°
T (K)	128 ± 5	116 ± 16	132 ± 8	133 ± 7	200 ± 13	142 ± 8	168 ± 10

early Earth's atmosphere before the buildup of oxygen 2.2×10^9 years ago (*9*).

During the Cassini spacecraft's first encounters with Titan, the Ion Neutral Mass Spectrometer (INMS) revealed an atmosphere dominated by N_2 and CH_4, accompanied by a rich mixture of hydrocarbon-nitrile compounds with masses up to 100 daltons (*10*), which was the upper detectable limit of the mass range of the INMS. Of particular importance for the development of complex chemistry in the upper atmosphere was the tentative identification of benzene (C_6H_6), which is a critical component in the formation of polycyclic aromatic hydrocarbon (PAH) compounds. In this paper, we report on quantitative observations of hydrocarbon-nitrile compounds in Titan's upper atmosphere (950 to 1150 km) by the INMS, together with evidence from the Cassini Plasma Spectrometer (CAPS) (*11*) of heavy positively charged (100 to 350 daltons) and negatively charged (20 to 8000 daltons) ions (*12*). The presence of negative ions in particular was a complete surprise, and we argue that they play an important role in tholin formation. These data were obtained during six recent Titan encounters (Tables 1 and 2), indicating that the chemical processes are a persistent phenomenon.

The low altitude (950 km) and high latitude (>70°) of the closest Cassini encounter with Titan (T16) allowed accurate determination of benzene density and mixing ratios over an altitude range of 130 km. Assuming local thermodynamic equilibrium with the major species (N_2), the fits to data (Fig. 1) give a scale height of ~15 km, which is consistent with a species with a molecular mass of 78 atomic mass units acting under molecular diffusion. This finding indicates that molecular diffusion, rather than turbulent atmospheric mixing, is the dominant transport process and that transport time scales are

Table 2. INMS observed ion densities (ions/cm^3) at closest approach. Ion data are not available for T20 because the ram-directed flow of ions during the encounter was outside the INMS field of view. LST, local solar time.

	T16	T17	T18	T19	T21	T23
CH_5^+	8.47×10^3 (1.03×10^4)	25.9 (0.977)	4.68 (0.600)	3.95×10^4 (9.93×10^3)	0.422 (0.272)	2.85×10^4 (4.88×10^4)
$C_2H_5^+$	2.83×10^4 (3.59×10^4)	153.0 (22.2)	13.75 (2.44)	2.18×10^5 (6.53×10^4)	1.09 (0.450)	1.35×10^5 (2.31×10^5)
$HCNH^+$	1.28×10^5 (1.62×10^5)	767 (85.8)	66.4 (10.4)	1.28×10^6 (3.01×10^5)	5.66 (3.24)	5.42×10^5 (9.28×10^5)
$C_3H_3^+$	1.12×10^5 (1.57×10^5)	113 (24.7)	71.7 (9.92)	7.51×10^5 (4.01×10^5)	41.9 (29.47)	2.41×10^5 (4.20×10^5)
$C_4H_3^+$	9.98×10^3 (1.73×10^4)	19.8 (9.95)	6.39 (0.903)	5.53×10^4 (5.55×10^4)	0.766 (0.216)	1.06×10^4 (1.99×10^4)
$C_4H_5^+$	9.05×10^3 (1.56×10^4)	14.8 (9.17)	7.26 (1.12)	3.52×10^4 (3.86×10^4)	1.09 (0.223)	1.15×10^4 (2.13×10^4)
$C_6H_5^+$	834 (2.10×10^3)	2.60 (2.70)	5.14 (0.763)	3.06×10^3 (4.98×10^3)	0.900 (0.755)	1.64×10^3 (3.88×10^3)
$C_6H_7^+$	1.04×10^3 (2.55×10^3)	3.80 (4.26)	5.83 (0.868)	3.61×10^3 (6.42×10^3)	0.504 (0.394)	2.22×10^4 (5.22×10^3)
$C_7H_7^+$	2.05×10^3 (3.40×10^3)	6.82 (8.33)	17.1 (2.30)	5.55×10^3 (9.33×10^3)	2.20 (1.96)	3.25×10^3 (7.40×10^3)
Altitude (km)	950	1000	960	980	1000	1000
LST	17.4	10.5	4.8	2.3	20.4	14.1

more rapid than chemical-loss time scales. Data taken during subsequent flybys have confirmed the presence of benzene at a mole fraction of ~1 to 5 parts per million (Table 1) and the dominance of transport in determining the altitude variation. INMS-derived ion and neutral spectra from 1 to 100 daltons (Fig. 2) illustrate the ion-neutral chemistry correspondence for compounds, starting with C1 compounds and continuing through benzene and toluene. In the case of benzene, a chemical equilibrium exists between it and the benzene cation $C_6H_7^+$. Other combinations of ion and neutral species seen in the spectra suggest the complexity of the chemical processes at work.

In addition to INMS data, the CAPS Ion Beam Spectrometer (IBS) (*11*) (Fig. 3A) found complex hydrocarbon-nitrile species at much higher molecular masses (~350 daltons) than can be measured by the INMS. However, whereas the INMS is a quadrupole mass spectrometer (*10*), the CAPS IBS is an electrostatic analyzer that makes use of the high Mach number (14 for a mass of 100 daltons) of cold ionospheric ions rammed into the instrument to infer mass/charge spectra from measured ion energy/charge and knowledge of the spacecraft's electrical potential in Titan's atmosphere. The IBS was not designed specifically for this task, and so its effective mass resolution at Titan is limited to a mass resolution ($M/\Delta M$, where M is the mass in daltons and ΔM is the mass resolution in daltons) of ~8 versus 100 for the INMS. However, IBS resolution is sufficient to separate families of mass peaks. This functionality is evident in the spectrum shown (Fig. 3A), where the unresolved mass groupings <100 amu correspond to families of peaks in the INMS spectra (Fig. 2). Of particular interest are several prominent peaks at ~130, ~170, and ~335 daltons. These we identify as naphthalene, anthracene derivatives, and an anthracene dimer.

The IBS analysis method can be applied to energy spectra (Fig. 3B) obtained from the CAPS Electron Spectrometer (ELS) (*11*, *12*) to infer the existence of heavy negative ions. Although designed to detect electrons, the ELS can also detect negatively charged ions. Analysis of the three-dimensional velocity distribution of the ions shows that, although extending to ~2 keV due to their kinetic energy in the moving spacecraft reference frame (6 km/s), the ions are very cold (~0.1 eV) and hence highly supersonic. Taking the energy spectra as proxies for mass spectra (Fig. 3B), we can identify peaks at ~15, ~35, and ~100 daltons and a broad range of masses between 100 and ~8000 daltons, with a peak at ~1500 daltons. Thus, both IBS and ELS data clearly show the presence of heavy molecules well above the mass range of the INMS, implying a complex organic chemistry that has neither been observed nor considered before.

The existence of large negative ions is an indication of complex carbon-nitrogen precursors (PAHs and assorted nitriles) that may lead to the production of tholins. Our analysis suggests that the organic compounds seen by the INMS and IBS are formed through ion-neutral chemical processes, which then give rise to the complex hydrocarbon-nitrile negative ions found by the ELS.

Earlier modeling efforts [for information on the initial model and revised ion-neutral chemistry added, see (*13*) and (*14*), respectively; for original references for benzene production, see (*6*–*8*)] showed that benzene can be produced by ion-neutral chemistry involving small molecules at altitudes near 1000 km in Titan's upper atmosphere and through three body–association reactions of carbon radicals near 750 km. INMS measurements (Fig. 2 and Tables 1 and 2) provide a direct means of evaluating high-altitude production pathways (Table 3). Although dissociation of methane and nitrogen is key to initiating the production of simple organic units (such as acetylene, ethylene, ethane, and hydrogen cyanide), ion-neutral chemistry must play a central role in linking these organic units together to form more complex organics, starting with benzene.

By untangling the complex hydrocarbon-nitrile mixture (*15*, *16*) that the INMS observes, we can estimate the chemical formation process for benzene using chemical schemes (Table 3) developed to understand the formation of soot on Earth (*6*–*8*, *13*, *14*) and PAHs in interstellar clouds (*17*). In the low-pressure regime found at ~1000 km, the ion-neutral formation pathway involving $C_4H_3^+$ and $C_4H_5^+$ is over five orders of magnitude faster than neutral reaction pathways acting through photochemical or energetic particle production of radical hydrocarbon species, such as C_2H. However, the photodissociation rate of benzene is large (>10^{-5} s^{-1}) and, when combined with the estimated ion-neutral production rate of 1×10^{-2} cm^{-3} s^{-1}, leads to the underestimation of the benzene concentration by about an order of magnitude. Potential solutions to this dilemma include (i) an unidentified benzene source at the altitude of observation, (ii) a stabilization or regeneration process that mitigates the photodissociation of benzene, or (iii) some combination of the two.

In addition to the measured benzene density profile (Fig. 1), independent evidence (*18*) indicates that the level at which molecular diffusion dominates turbulent mixing is over two scale heights below 1000 km. We calculate a transport lifetime based on the molecular diffusion coefficient (*14*) of 5×10^5 s, which is to be compared with the chemical loss lifetime of 1×10^5 s. Thus, the photodissociation pathway cannot be representative of the chemical lifetime. An alternative involves rapid regeneration of benzene after dissociation to the C_6H_5 or C_6H_4 radicals. Most of the obvious reactive pathways involving reactions with H_2, CH_4, C_2H_2, C_2H_4, or C_2H_6 have activation energies (*19*, *20*) that render these reactions ineffective in the low temperature (120 to 130 K) of Titan's atmosphere (near 1000 km) in high northern latitudes, whereas pathways that involve growth to more complex organics proceed with lower activation energies and therefore more rapid reaction rates. Therefore, we conclude that the

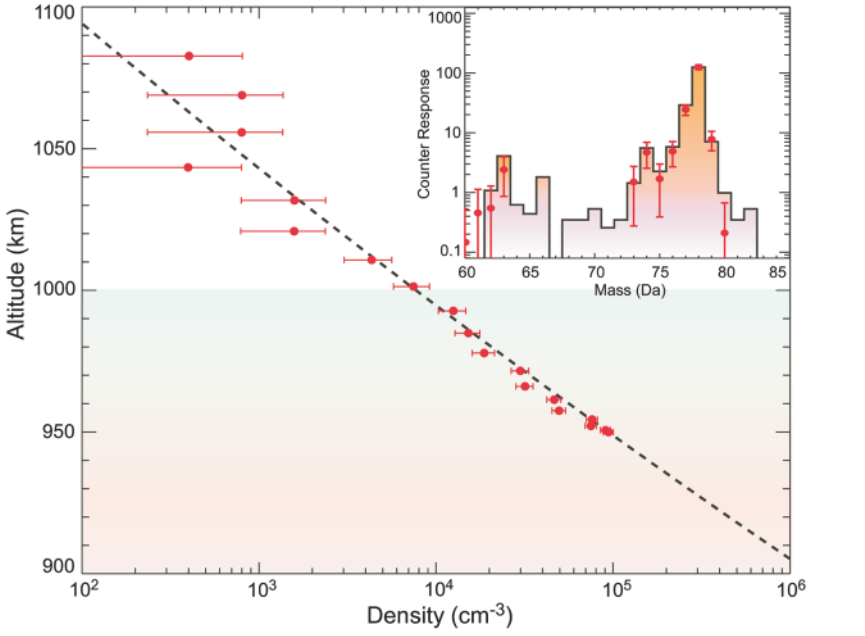

Fig. 1. INMS measurements of the altitude distribution of benzene during the T16 Titan encounter. Error bars indicate statistical uncertainty in counting rates. The dashed line is an exponential fit to the data, indicating the molecular diffusive scale height of a molecule the mass of benzene in Titan's atmosphere. Data below 1000 km (blue region) were averaged to produce the mass spectrum shown in the inset. (**Inset**) Fits to the benzene mass spectrum with the use of recent INMS calibration values are shown, along with estimated uncertainty (error bars).

ultimate fate of benzene dissociation is the production of higher-order PAHs and that diffusive mixing inferred from the observed altitude distribution requires a loss rate through photodissociation that is an order of magnitude slower than present measurements and theories suggest [for rates used, see (*21*); see also (*22*) and, for dissociation products, (*23*–*25*)]. Indeed, this is consistent with the measured benzene concentration based on our present inferences of chemical production rates. Model calculations (*14*) suggest that production at smaller solar-illumination angles rises at a rate that compensates for increased losses from photodissociation, and therefore the benzene concentration may remain the same in the illuminated upper atmosphere (T17 in Tables 1 and 2). Our present observations thus leave open the questions of missing benzene production mechanisms and stabilization of the "hot" benzene formed through photodissociation.

Our data show that the key chemical role of benzene-PAH formation begins at high altitudes. CAPS IBS measurements (Fig. 3A) allow us to tentatively infer the existence of higher-order PAH ions associated with higher-order PAHs, such as naphthalene (~130 daltons) and anthracene (~170 daltons). Furthermore, comparison of measured densities with the saturation vapor pressure (*26*) shows that benzene and hydrogen cyanide are near saturation vapor pressure and that diacetylene, naphthalene, and anthracene are highly supersaturated at 125 K (Table 1). This comparison is reinforced by the tentative identification of ions associated with the anthracene dimer near 340 daltons as measured by the IBS. The decreasing density of the intervening species between 170 and 340 daltons suggests a competition between chemistry and physical condensation processes. Dimer formation is the first step in condensation in the free molecular flow regime, where bimolecular reactions dominate the condensation formation process (*27*) and competing condensation and chemical kinetics are a hallmark of existing soot formation models (*6*–*8*). From the measured ion densities, we infer the relative rate of condensation to be one-tenth that of chemical processes. We also estimate a production rate ($>1 \times 10^{-16}$ g cm^{-2} s^{-1}) for formation of more complex PAH-nitrile compounds from benzene.

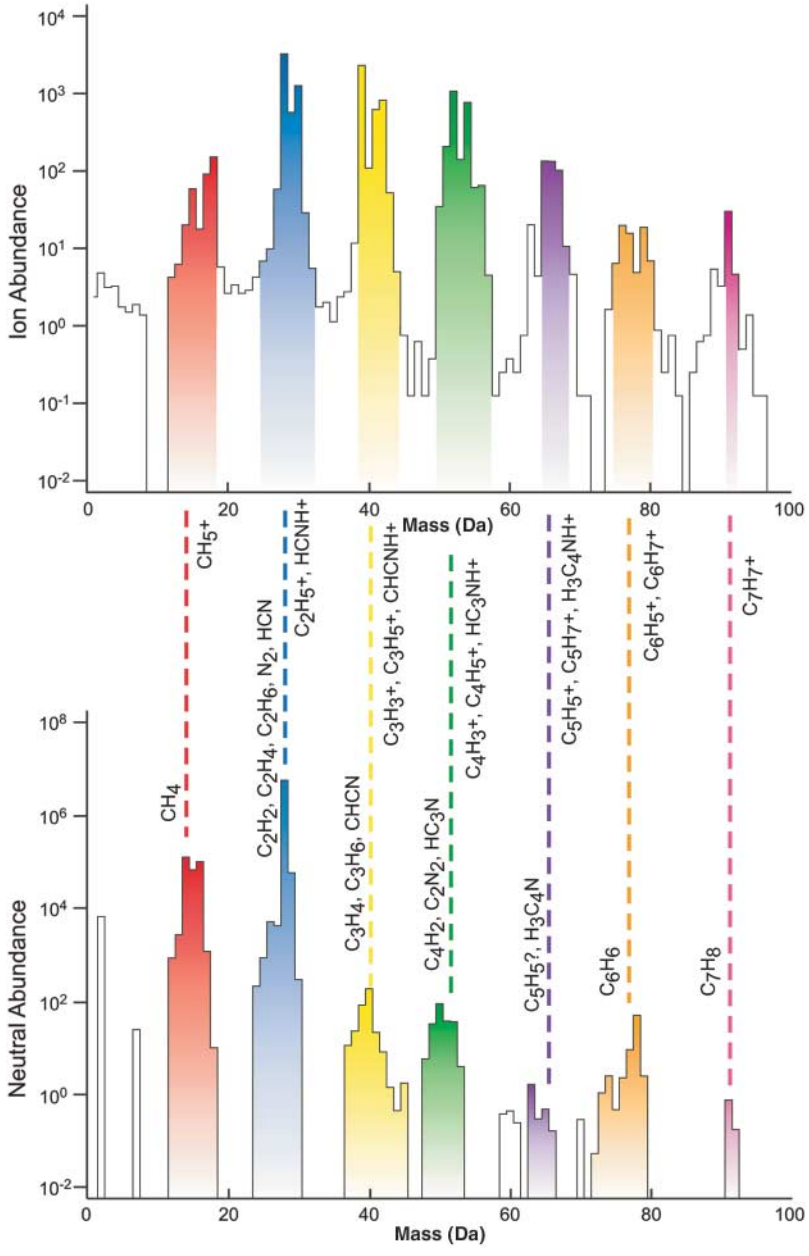

Fig. 2. Correspondence of ion (**upper**) and neutral (**lower**) mass spectra measured by INMS during T19 between 950 and 1000 km. Benzene molecules and their ion counterpart can be identified at 78 and 79 daltons in the spectra. High-pressure background in the ion source has been subtracted from the neutral spectrum.

The final step in the tholin formation process is aggregation of higher-order PAH-nitrile compounds that lead to negative ions. Negative ion formation is expected as a result of the tendency of complex PAHs and cyanoaromatics (*28*, *29*) to have electron affinities that range between 2 and 5 eV. Our observations of ions with mass/charge (amu per atomic charge e) between 1000 and 8000 daltons (Fig. 4) suggest that this is indeed occurring. Under the conditions at ~1000 km (T_e = ~125 K and n_e = ~10^9 m^{-3}, where T_e is electron temperature and n_e is electron density), small dust grains immersed in a plasma will charge negatively to a potential (*30*) $\varphi \sim -2.5$ kT/e ~ −0.027 V with a charge $Q = 4\pi\varepsilon_0 a \varphi \exp(-a/\lambda_D)$, where ε_0 is the permittivity of free space, a is the particle radius, and λ_D is Debye length. If we assume the ions are singularly charged with a density of 1×10^{-3} kg m^{-3}, then the particle radius lies between 75 and 150 nm. Because we cannot measure charge independently, the ion mass may actually be much larger. A particle with mass/charge of 8000 daltons, an assumed density of 1×10^{-3} kg m^{-3}, and Q = 5e has a mass of 40,000 amu and a radius of 260 nm. These particles are clearly the size of aerosols that, because of the chemical processes taking place around them, we identify as tholins. Particles of this size are gravitationally bound to Titan and will tend to sink into the lower atmosphere, where they are indeed found (*3*, *4*). The interactions of these charged tholins with ambipolar (*31*) and induced corotational (*31*) electric fields remain to be investigated. Depending on the influence of the electric fields, the charged tholins may descend into the stratosphere or escape Titan's atmosphere altogether.

Other instrumentation aboard the Cassini spacecraft is providing corroborating evidence of high-altitude aerosols. The Cassini Ultraviolet Spectrometer (UVIS) has recently observed aero-

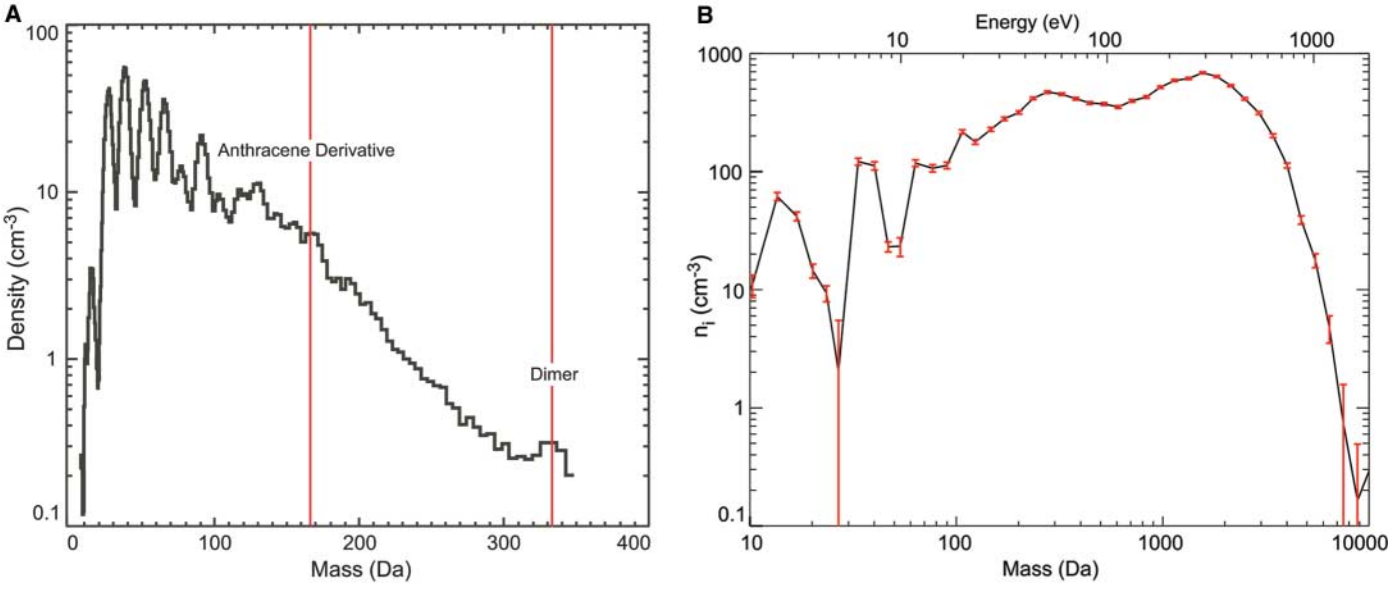

Fig. 3. (**A**) Positive ion spectrum from 1 to 350 daltons inferred from energy/charge measurements made by the CAPS IBS near 1000 km during the T18 encounter. There is a change in slope of the ion abundance near 170 daltons and a change in the appearance of peaks near 170 and 340 daltons. These appear to be an indication of the onset of condensation of the complex carbon-nitrogen aromatics. (**B**) Negative ion (n_i) spectrum from 10 to 10,000 daltons inferred from energy/charge measurements made by the CAPS ELS near 1000 km during the T16 encounter. Error bars indicate uncertainty in the number density.

Table 3. The primary ion and neutral chemical reactions in Titan's atmosphere at ~1000 km (*37*–*40*). *k*, chemical rate coefficient; *hυ*, photonic energy; -, not measured. The asterisk indicates that the reaction occurs at 125 K.

Formation of	Relevant reaction(s)	*k* (cm^3 s^{-1})
$C_4H_3^+$	$C_4H_2 + C_2H_5^+$, $HCNH^+$, $CH_5^+ \rightarrow C_4H_3^+ +$ products	-
$C_4H_5^+$	$C_2H_2 + C_2H_5^+ \rightarrow C_4H_5^+ + H_2$	-
$C_6H_7^+$	1. $C_4H_5^+ + C_2H_4 \rightarrow C_6H_7^+ + H_2$	7.3×10^{-11}
	2. $C_4H_3^+ + C_2H_4 \rightarrow C_6H_5^+ + H_2$	1.2×10^{-10}
	(followed by) $C_6H_5^+ + H_2 \rightarrow C_6H_7^+ + h\upsilon$	3.0×10^{-11}
	(or) $C_6H_5^+ + C_2H_4 \rightarrow C_6H_7^+ + C_2H_2$	1.7×10^{-11}
	(which competes with) $C_6H_5^+ + CH_4 \rightarrow C_7H_7^+ + H_2$	7.5×10^{-11}
	(which recombines to form benzene) $C_6H_7^+ + e \rightarrow C_6H_6 + H$	1.5×10^{-6}*

sols at an altitude of 1000 km (*32*). They suggest that Mie scattering from particles with radii of 12.5 nm with number densities of ~50 cm^{-3} provides an adequate explanation of the data. The size that UVIS infers for the aerosols is to be compared to the mass/charge group detected at 8000 daltons by the CAPS ELS. Each of these particles is interpreted as having a mass of 40,000 amu, a density of 1×10^{-3} kg m^{-3}, and a size of 260 nm. However, the CAPS-inferred densities are lower than those acquired by the UVIS, albeit at a very different time and place.

Benzene and higher-order PAH production at high altitudes is indicative of additional complex chemistry involved in the growth of tholins at lower, stratospheric altitudes. Evidence identifying the existence of benzene in the troposphere (*33*) and stratosphere (*4*) also suggests that benzene plays a major role in the growth of tholins throughout the atmosphere. Benzene has been observed to vary with latitude in the stratosphere, with mixing ratios of 5×10^{-10} in the south and a maximum of 3×10^{-9} in the north at 75°N (*4*). Low temperatures (120 to 130 K) measured at high northern latitudes in the upper atmosphere near 1000 km result in near saturation pressures for benzene and hydrogen cyanide and highly supersaturated conditions for diacetylene, naphthalene, and anthracene (*26*). This promotes rapid tholin growth through heterogeneous condensation (*27*) and internal particulate chemistry (*6*–*8*, *17*, *27*) and leads to a transfer of benzene and other organics from the gas phase to the surface of the tholins. The loss of benzene and other compounds through condensation onto the nascent tholin may account for the observation that benzene mixing ratios observed in the thermosphere are more than four orders of magnitude larger than those in the stratosphere.

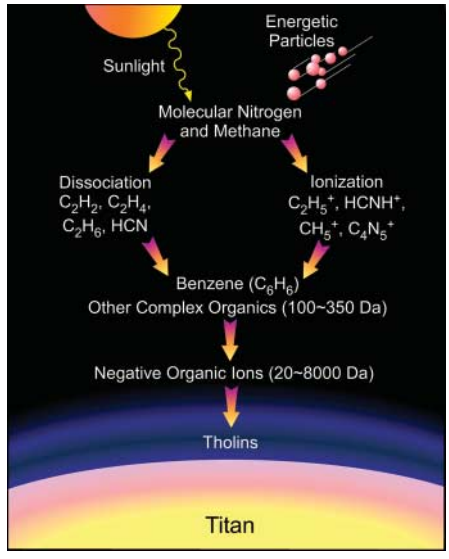

Fig. 4. Cartoon showing the chemical process leading up to the formation of tholins in Titan's upper atmosphere. The process begins with free energy from solar UV radiation and energetic particles impinging on Titan's atmosphere. The most abundant constituents (CH_4 and N_2) combine through a number of reaction pathways to form larger organic and nitrile compounds (100 to 350 daltons) that eventually lead to the formation of negatively charged tholin aerosols (20 to 8000 daltons) observed at ~1000 km.

We have presented data from three Cassini particle spectrometers that indicate that a complex ion-neutral chemistry in Titan's atmosphere near 1000 km plays a major role in the formation

of progressively more complex hydrocarbon molecules, from benzene to PAHs and ultimately to aerosol particles with ~260-nm radii. The existence of ~40,000-amu aerosols, formed by the growth of complex organic compounds in the upper atmosphere, appears to answer the long-unresolved question of the origin of tholin precursors found at Titan. The chain of molecular growth that we have identified in this study is similar to that first identified in the Miller-Urey experiments (*3*). We suspect that the ultimate destination of these large organic molecules and aerosols lies in the organic haze layers in Titan's stratosphere (*3*, *4*). However, depending on the dynamic effects of atmospheric and induced co-rotational electric fields on these particles, they might also escape Titan's atmosphere to become the source of PAHs observed to collect on the surfaces of Saturn's icy moons (*34*, *35*).

References and Notes

1. R. V. Yelle *et al.*, *Icarus* **72**, 468 (2006).
2. Y. L. Yung, M. Allen, J. P. Pinto, *Astrophys. J. Suppl. Ser.* **55**, 465 (1984).
3. C. Sagan, B. N. Khare, *Nature* **277**, 102 (1979).
4. C. P. McKay *et al.*, *Planet. Space Sci.* **49**, 79 (2001).
5. A. Coustenis *et al.*, *Icarus*, in press; available online at http://dx.doi.org/10.1016/j.icarus.2006.12.022.
6. H. Richter, J. B. Howard, *Prog. Energy Combust. Sci.* **26**, 565 (2000).
7. H. F. Calcote, D. G. Keil, *Pure Appl. Chem.* **62**, 815 (1990).
8. M. Frenklach, *Phys. Chem. Chem. Phys.* **4**, 2028 (2002).
9. A. A. Pavlov, M. T. Hurtgen, J. F. Kasting, M. A. Arthur, *Geology* **31**, 87 (2003).
10. J. H. Waite Jr. *et al.*, *Science* **308**, 982 (2005).
11. D. T. Young *et al.*, *Space Sci. Rev.* **114**, 1 (2004).
12. A. J. Coates *et al.*, *Eos Trans. Am. Geophys. Union* **87** (fall meeting suppl.), 52, abstract P21B-06 (2006).
13. E. H. Wilson, S. K. Atreya, A. Coustenis, *J. Geophys. Res. (Planets)* **108**, 5014 (2003).
14. V. De La Haye, thesis, University of Michigan, Ann Arbor, MI (2005).
15. T. E. Cravens *et al.*, *Geophys. Res. Lett.* **32**, L12108 (2005).
16. V. Vuitton, R. V. Yelle, V. G. Anicich, *Astrophys. J.* **647**, L175 (2006).
17. D. K. Bohme, *Chem. Rev.* **92**, 1487 (1992).
18. All minor neutral constituents (with the exception of methane) show molecular diffusive scale heights at our lowest altitude on T16, most notably the inert species ^{40}Ar. We can use the mixing ratio of ^{40}Ar measured in the lower atmosphere by the Huygens Gas Chromatograph Mass Spectrometer [4.32×10^{-5} (*33*)] and the ^{40}Ar mixing ratio measured by the INMS on T16 at 975 km of $1.46 \times 10^{-5} \pm 0.14 \times 10^{-5}$ to infer that the homopause or turbulent mixing boundary lies ~110 km below our observation point (865 ± 25 km), where the altitude uncertainty represents uncertainties in the atmospheric temperature profile and the mixing ratio of ^{40}Ar. The lack of compliance of methane with a molecular diffusive scale height has been suggested as due to outflow (*1*, *2*).
19. National Institute of Standards and Technology (NIST) Chemical Kinetics Database (www.kinetics.nist.gov/kinetics/index.jsp).
20. I. V. Tokmakov *et al.*, *J. Phys. Chem. A* **103**, 3636 (1999).
21. J. Crovisier, *J. Geophys. Res.* **99**, 3777 (1994).
22. J. I. Moses *et al.*, *J. Geophys. Res.* **110**, e08001 (2005).
23. A. Yokoyama *et al.*, *J. Chem. Phys.* **92**, 4222 (1990).
24. K. Shindo, S. Lipsky, *J. Chem. Phys.* **45**, 2292 (1966).
25. N. Nakashima, Y. Keitaro, *J. Chem. Phys.* **79**, 2727 (1983).
26. We calculated vapor pressure (P) values using the Antoine equation [$\log P = A - B/(T + C)$] and the parameters A, B, and C using experimental data in a specific temperature (T) range. The extrapolation of these data by means of the Antoine equation to lower temperatures has been verified with the use of benzene and methane data. We performed a verification by producing a test case where the Antoine equation fit was produced using only the high-temperature values, which we then compared with the experimental low-temperature data. Our test case shows a maximum uncertainty of one decade at the extreme low temperatures (less than 100 K) and, at 130 K, the extrapolated data differ by a factor of five. The parameters A, B, and C are obtained from (*36*).
27. A. J. Friedson, A.-S. Wong, Y. L. Yung, *Icarus* **158**, 389 (2002).
28. T. Moustefaoui *et al.*, *Faraday Discuss. Chem. Soc.* **109**, 71 (1998).
29. X. Zhang *et al.*, *Chem. Commun.* **2006**, 758 (2006).
30. C. K. Goetz, *Rev. Geophys.* **27**, 271 (1989).
31. M. G. Kivelson, C. T. Russell, Eds. *Introduction to Space Physics* (Cambridge Univ. Press, Cambridge, 1995).
32. M.-C. Liang, Y. L. Yung, D. E. Shemansky, paper presented at the 38th Annual Meeting of the Division of Planetary Sciences, American Astronomical Society, Pasadena, CA, 8 to 13 October 2006.
33. H. B. Niemann *et al.*, *Nature* **438**, 779 (2005).
34. D. P. Cruickshank *et al.*, *Icarus*, in press.
35. R. N. Clark *et al.*, *EOS Trans. Am. Geophys. Union*, **87** (fall meeting suppl.), abstract P32A-03 (2006).
36. P. J. Linstrom, W. G. Mallard, Eds. *The National Institute of Standards and Technology Chemistry WebBook* (NIST Standard Reference Database Number 69, June 2005 release); (http://webbook.nist.gov/chemistry/).
37. J. L. McLain, V. Poterya, C. D. Molek, L. M. Babcock, N. G. Adams, *J. Phys. Chem. A* **108**, 6704 (2004).
38. V. G. Anicich, "An index of the literature for bi-molecular gas-phase-cation-molecule reaction kinetics" (NASA Jet Propulsion Laboratory, JPL Publication 03-19, Pasadena, CA, 2003).
39. V. G. Anicich, M. McEwan, *Planet. Space Sci.* **45**, 897 (1997).
40. V. G. Anicich, P. F. Wilson, M. J. McEwan, *J. Am. Soc. Mass Spectrom.* **17**, 544 (2006).

41. We thank NASA for its continuing support of operations and data analysis from the Cassini mission and A.J.C. thanks the Science and Technology Facilities Council for support of ELS. The INMS and CAPS teams acknowledge support from NASA and the Jet Propulsion Laboratory (SWRI subcontract numbers 1283095 and 1243218, respectively), as well as the support of their respective science and operations teams. J.H.W. acknowledges numerous helpful discussions with G. R. Gladstone, and A.J.C. acknowledges help with the data analysis from G. R. Lewis.

9 January 2007; accepted 26 March 2007
10.1126/science.1139727

The Orientation of the Local Interstellar Magnetic Field

M. Opher,[1]* E. C. Stone,[2] T. I. Gombosi[3]

The orientation of the local interstellar magnetic field introduces asymmetries in the heliosphere that affect the location of heliospheric radio emissions and the streaming direction of ions from the termination shock of the solar wind. We combined observations of radio emissions and energetic particle streaming with extensive three-dimensional magnetohydrodynamic computer simulations of magnetic field draping over the heliopause to show that the plane of the local interstellar field is ~60° to 90° from the galactic plane. This finding suggests that the field orientation in the Local Interstellar Cloud differs from that of a larger-scale interstellar magnetic field thought to parallel the galactic plane.

The heliosphere created by the supersonic solar wind is compressed by the motion of the Sun relative to the local interstellar medium, producing a comet-like shape with an extended tail. The solar wind abruptly slows, forming a termination shock as it approaches contact with the interstellar medium at the heliopause. Beyond the heliopause, the interstellar wind contains mainly hydrogen and helium, both as neutral atoms and as ions that carry the frozen-in interstellar magnetic field.

Recent Voyager observations of ions streaming from the termination shock (*1*, *2*) have led to the suggestion that north-south and east-west asymmetries of the heliosphere are induced by the interstellar magnetic field (*3*). However, the inferred field direction from the model of (*3*) was parallel to the hydrogen deflection plane (HDP) rather than the galactic plane (GAL). On the basis of the polarization of light from nearby stars, Frisch (*4*, *5*) suggested that the galactic magnetic field is parallel to the GAL. However, the direction of the galactic magnetic field is deduced from measurements averaged over a much larger distance (light-years). A direction parallel to the HDP was suggested by Lallement *et al.* (*6*) for the local interstellar field, on the basis of solar Lyman-α radiation that is resonantly backscattered by interstellar hydrogen atoms. The HDP is tilted from the ecliptic plane by 60° and differs from the GAL by 60°. We used Voyager 1 and 2 observations in conjunction with a magnetohydrodynamic model to discriminate between these two planes and to constrain the orientation of the local interstellar magnetic field.

[1]Department of Physics and Astronomy, George Mason University, 4400 University Drive, Fairfax, VA 22030, USA. [2]California Institute of Technology, Pasadena, CA 91125, USA. [3]Center for Space Environment Modeling, University of Michigan, Ann Arbor, MI 48109, USA.

*To whom correspondence should be addressed. E-mail: mopher@physics.gmu.edu